The Climatology of Explosive Cyclogenesis in Two General Circulation Models

FREDERICK SANDERS
Marblehead, Massachusetts

STEVEN L. MULLEN
Institute of Atmospheric Physics, University of Arizona, Tucson, Arizona

(Manuscript received 7 November 1995, in final form 14 March 1996)

ABSTRACT

The occurence of explosive cyclogenesis is studied in two 180-day cold-season simulations by the Community Climate Models (CCM1 and CCM2) developed at the National Center for Atmospheric Research. The CCM1 run was realistic in some respects but produced relatively few cases over the North Atlantic Ocean and failed to show concentration just off the east coasts of the continents and north of the warm ocean currents. The intensity of cyclogenesis was underestimated in the CCM1 run. All of these flaws were mended in the CCM2 run, in which the climatology of explosive cyclogenesis closely resembled that in the real atmosphere.

1. Introduction

As a basis for selecting cases of explosive cyclogenesis (Sanders and Gyakum 1980, hereafter SG) to be studied as examples of ensemble forecasting, we have examined 180-day runs of Community Climate Models (CCM) 1 and 2 (Williamson et al. 1987; Hack et al. 1993, respectively), two general circulation models of the National Center for Atmospheric Research (NCAR). By doing this, we hope to avoid the uncertainty associated with the sparcity of observations over the oceans of midlatitudes. To be successful in this effort, the models must be capable of simulating explosive cyclogenesis as it is known to occur in the real atmosphere.

2. Model description

Both the CCM1 and CCM2 use the spectral transform method for horizontal derivatives and linear operations. At each vertical level, the dependent variables are represented as series of spherical harmonic functions. The vertical component of vorticity and the horizontal divergence serve as prognostic variables for the horizontal wind field. The continuity equation and predictive equations for temperature and water vapor mixing ratio close the system of prognostic equations. The spectral resolution, for both models, is triangular 63 (T63). This resolution provides 96 Gaussian latitudes between the poles and 192 grid points along each latitude. The equivalent gridpoint resolution is about 1.8° of latitude and longitude, and the smallest resolvable wavelength is about 500 km. The coarseness of the Gaussian grid in a spectral model, relative to a gridpoint model, is compensated by the elimination of aliasing in the computations.

Temporally, a semi-implicit leapfrog scheme is used with a time step of 12 min. Both models use a linear ∇^4 form of horizontal diffusion applied directly to model surfaces in the stratosphere and a linear ∇^4 form with a partial correction for diffusion along isobaric surfaces in the troposphere. Nonlinear dynamics and parameterizations are performed on the 96 × 192 latitude–longitude transform grid.

The CCM1 employs a terrain-following sigma vertical coordinate with 12 layers, seven of which are situated below the 200-mb level. The top of the highest model layer is at 0 mb. The vertical coordinate in the CCM2 is a hybrid sigma-pressure system. Here the four layers above 83.1425 mb blend smoothly with the terrain-following sigma coordinate, with only the lowest layer being purely sigma. The model top for the CCM2 is set at 2.917 mb. Of the total of 18 vertical layers, 11 are located below 200 mb. The CCM2 employs a shape-preserving semi-Lagrangian method of transporting water vapor that prevents the occurrence of negative mixing ratios.

Both models include the following parameterized physical processes: convection; condensation; shortwave and longwave radiative transfers; surface fluxes of heat, moisture, and momentum; and interaction with subgrid-scale motions through diffusion. Clouds are formed in the model and can be of either convective or stratiform type. They are radiatively active. In midlat-

Corresponding author address: Dr. Frederick Sanders, 9 Flint Street, Marblehead, MA 01945.

TABLE 1. Summary of primary differences in physical parameterizations between CCM1 and CCM2.

Process	CCM1	CCM2
Moist convection	Moist convective adjustment Manabe et al. (1965)	Three-layer mass-flux scheme (Hack 1993)
Planetary boundary layer	Bulk aerodynamic	Nonlocal PBL Scheme (1990)
Radiative transfer	Kiehl et al. (1987)	Hack et al. (1993)

itudes, clouds are allowed in all tropospheric layers except the lowest one. If the relative humidity exceeds 100% clouds are formed and the excess water vapor is precipitated without evaporation of the condensate in the layers below. Aside from the finer vertical resolution in the CCM2, the models differ most importantly in some of the physical parameterizations, as specified in Table 1.

Sea surface temperature, sea-ice distribution, and snow cover are externally prescribed and vary in accordance with the long-term seasonal averages. Incoming solar radiation varies daily according to a solar year of 365 days, and the earth's orbital parameters are set to their current values. The CCM2, but not the CCM1, also contains a diurnal variation in insolation, with full radiation calculations performed every hour. Both models include a smoothed spectrally analyzed T63 representation of the earth's orography.

The two simulations studied in this work each cover a single cool season, defined as the six months beginning 1 October. For the CCM1 the output is available once daily from case 263, an experimental simulation run for less than one year (D. L. Williamson 1955, personal communication). The cool season examined for the CCM2 is the first of a 20-yr control simulation, case 388 (Williamson 1993). Twice-daily output for this cool season was made available through the kindness of D. Baumhefner. Both simulations were initialized from analyses for 0000 UTC 1 October 1975.

More detailed accounts of the CCM1 and CCM2 formulations are provided by Williamson et al. (1987) and by Hack et al. (1993), respectively. The purpose of this paper is to determine the occurrence of explosive cyclogenesis in these model atmospheres and to compare with the occurrence in the observed atmosphere, as presented by SG in their study of three cold seasons.

To determine the model's verisimilitude with respect to explosive cyclogenesis, instances were tabulated through use of the criterion established by SG. In particular, for inclusion the central pressure of the cyclone was required to drop at least 24 mb in 24 h (multiplied by the ratio of the sine of the storm's central latitude to the sine of 60°). This critical deepening is assigned the value of 1 bergeron. Generally, the bergeron number for a given cyclone during a given 24-h period is

$$b = \frac{\text{24-h deepening (mb)}}{\text{24-mb } [(\sin L/\sin 60)]},$$

where L is the latitude of the low center at the midtime of the 24-h interval. The aspects of explosive cyclogenesis with which we will be concerned comprise frequency, location, and intensity.

3. The CCM1 simulation

The locations of the qualifying cyclones found over the Pacific and Atlantic sectors in the CCM1 model run are shown in Figs. 1a and 1b, respectively. The total

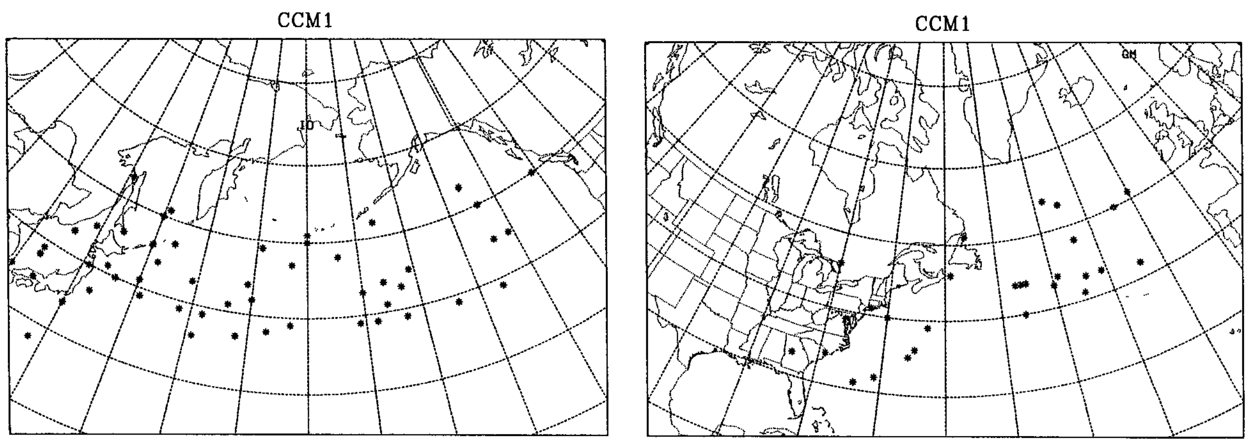

FIG. 1. Location of explosively deepening cyclones at midpoint of 24-h period of intensification in the CCM1 simulation. (a) Pacific sector, (b) Atlantic sector.

number of cases in the model run is 79, with 52 Pacific events and 17 over the Atlantic. As in SG, overland cases are restricted to a few in eastern North America. SG found, during three cold seasons (averaging 198 days duration), 155 instances in the Pacific sector and 109 over the Atlantic, an average of 88 for a single season over the combined sectors. Aside from failure to replicate a pronounced maximum near 40°N, 150°E, one could hardly find fault with the frequency of Pacific explosive cyclogenesis in the model, but there appears to be a substantial model shortfall over the Atlantic.

The march of monthly frequency in the CCM1 resembled that in SG's study (see their Fig. 4). The peak is slightly earlier, near 0.8 per day in "December and January" (days 60–120), and there is a sharper decrease toward the end of the period.

Comparison of Fig. 1 with SG's Fig. 3 shows generally good agreement in location of explosive cyclogenesis. The most noticeable discrepancy in the model results is the failure in the Atlantic to produce a maximum southeast of the Canadian Maritimes and north of the Gulf Stream, and in the Pacific to produce the intense maximum just east of Japan and north of the Kuroshio.

As to intensity, there is a substantial difference. Only three model cases reached 2 bergerons (about 4% of all cases), and none were seen in the Atlantic sector. In contrast, SG found 21 2-bergeron events in 267 cases (about 8%). The most intense case in SG showed 2.8 bergerons, although in other years individual storms deepened in excess of 3.0. The extreme case in the CCM1 simulation was a less spectacular 2.2.

4. The CCM2 simulation

The locations of 193 cases of explosive cyclogenesis in the CCM2 run are shown in Fig. 2. The large number of events reflects the twice per day in which they were sought. Since roughly equal numbers of events occurred in the 24-h periods ending at 0000 and 1200 UTC, one-half of the number in this simulation should be compared with SG's frequencies noted above. The 96 events thus obtained for the CCM2 run are in very good agreement with the 88 per cool season found by SG. The CCM2 run eliminates the shortfall in the Atlantic Basin seen in the CCM1 run, producing only somewhat fewer cases there than in the Pacific region. The difference between the percentage of Pacific cases versus Atlantic cases was far from being significant at the 5% level, according to a normal test (Wadsworth and Bryan 1960, 614–617).

Figure 2 shows that the location of events, as in the CCM1 run, was over maritime regions, with only a handful over eastern North America. Unlike the CCM1 run, concentrations of cases are seen just southeast of the Canadian Maritimes and east of the Japanese islands, as in SG. It appears that the CCM2 displays explosive cyclogenesis slightly too far north, but the discrepancy is small. A cursory study of the mean 500-mb flow in the model and in the observations suggests that the maximum wind in the western Pacific and western Atlantic is also slightly farther north in the model than in the observations.

The monthly march of CCM2 cases appears in Fig. 3, with account taken of the twice-daily output. There is a peak in mean daily frequency in "December," whereas SG found a maximum in January (their Fig. 4). There is a broad maximum from "November" through "February," with notably lower frequencies at the beginning and end of the 180-day simulation period.

So far as intensity is concerned, the CCM2 closely matches the SG results. The 24 cases of $b \geqslant 2.0$ (12.4%) in the CCM2 run is almost identical to the 21 cases (7.9%) found in the SG sample. The extreme cases are 2.8 bergerons in SG and 3.1 in the CCM2 results. To test the significance of the differences between the CCM2 and SG distributions of deepening

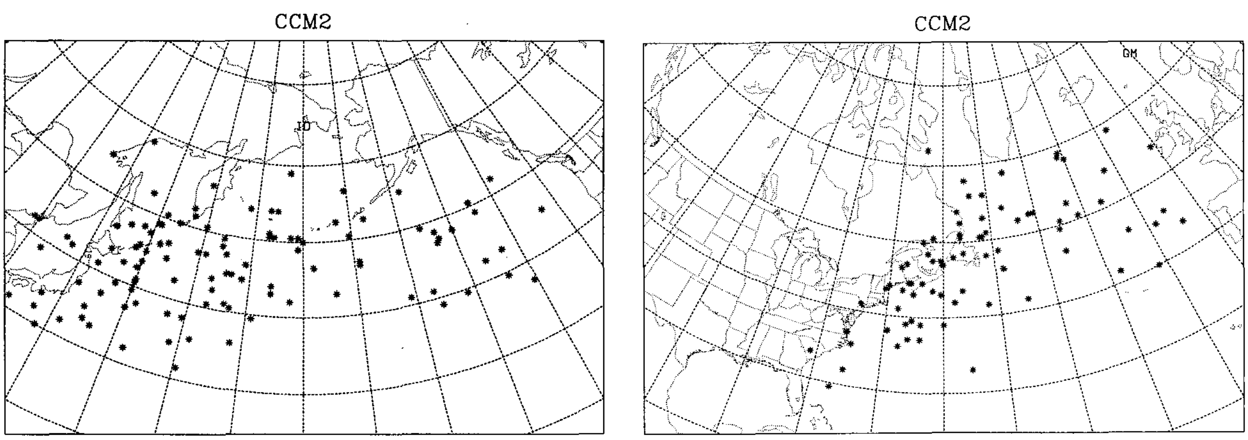

FIG. 2. Same as in Fig. 1 but for the CCM2 simulation.

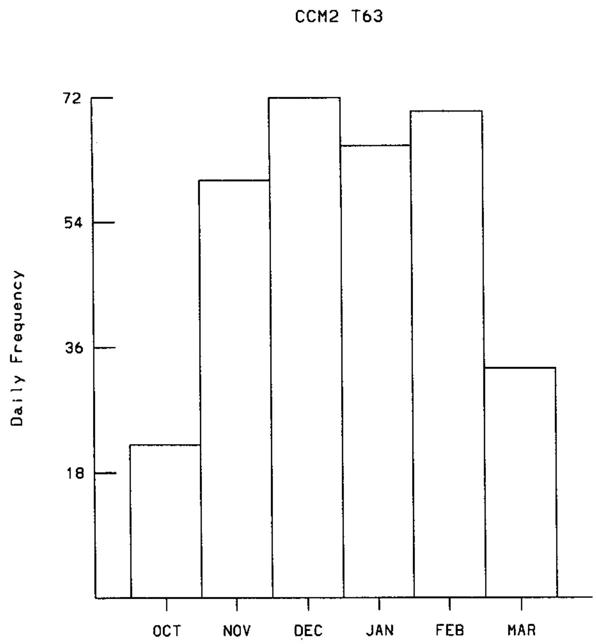

FIG. 3. March through the cold season of mean daily frequency of explosive cyclogenesis in the CCM2 run. "October" is identified with days 0–30, "November" with days 30–60, etc. Compare with SG's Fig. 4.

rate and the monthly distributions, we used the chi-square test for two binned datasets (Press et al. 1992, 614–617). Neither difference was close to being significant at the 5% level.

Very intense gradients of sea level pressure were noted over the high elevations of southern Asia, with pressures generally much lower at 0000 UTC than at 1200 UTC. Any 24-h changes that might have met our criterion for explosive cyclogenesis were disregarded because such changes must have reflected strongly the arbitrary reduction of surface pressure to sea level. It is our understanding that only the current temperature in the lowest model layers are used in this reduction. Therefore, the warmer temperatures at 0000 UTC, rather than 12 h earlier or later, were responsible for the large diurnal changes in reduced sea level pressure.

We can only speculate concerning the reasons for the improvement of CCM2 over CCM1 in the simulation of explosive cyclogenesis, and we admit some surprise since the horizontal resolution of the two models is the same. Candidates for responsibility for improvement are the increased vertical resolution and the improved treatment of the fluxes at the surface, as well as an improved cumulus parameterization.

Since there is a certain interannual variability in the observed atmosphere and no doubt also in seasonal simulations, we conclude that the climatology of explosive cyclogenesis in this last run closely resembles the climatology in the observations. The CCM2 run can be used with confidence, then, in the selection of cases for ensemble experiments.

5. An extreme example

To see whether cyclogenesis in the model proceeds as in the real atmosphere, we present sea level and 500-mb charts for the second strongest event, which achieved 2.9 bergerons. This system originated on day 98 as a trough in the geostrophic easterlies in the vicinity of the Philippine Islands (not shown), while a trough of extremely cold air occupied northern central Asia.

By day 101 (Fig. 5a) the low appeared as a 1007-mb center over the Japanese Island of Kyushu, close on the heels of a 994-mb low east of Sakhalin (also an explosive deepener, although marginal). At 500 mb (Fig. 5b) a pronounced vorticity center over northern Korea, about 1000 km west of the surface cyclone over Japan, had become organized in the base of the cold trough. In the following 24 h, the surface low deepened 54 mb (Fig. 6a) while moving east-northeastward at about 25 m s^{-1}. At 500 mb the vorticity center also intensified while moving even faster, becoming nearly coincident with the surface center (Fig. 6b). This relative motion of the surface and upper features was shown by Sanders (1986) to be typical of explosive cyclogenesis.

Even after the system had become nearly vertical, the cyclone deepened another 19 mb in the ensuing

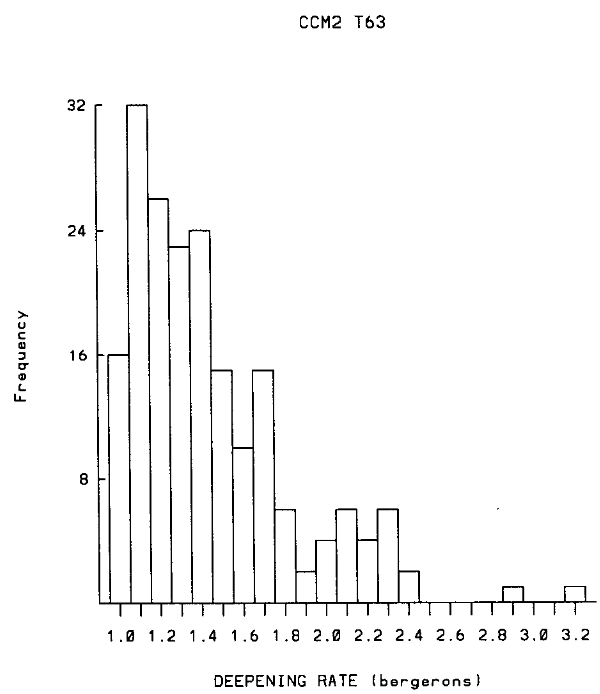

FIG. 4. Frequency of cases with indicated deepening rate, in bergerons. Compare with SG's Fig. 5.

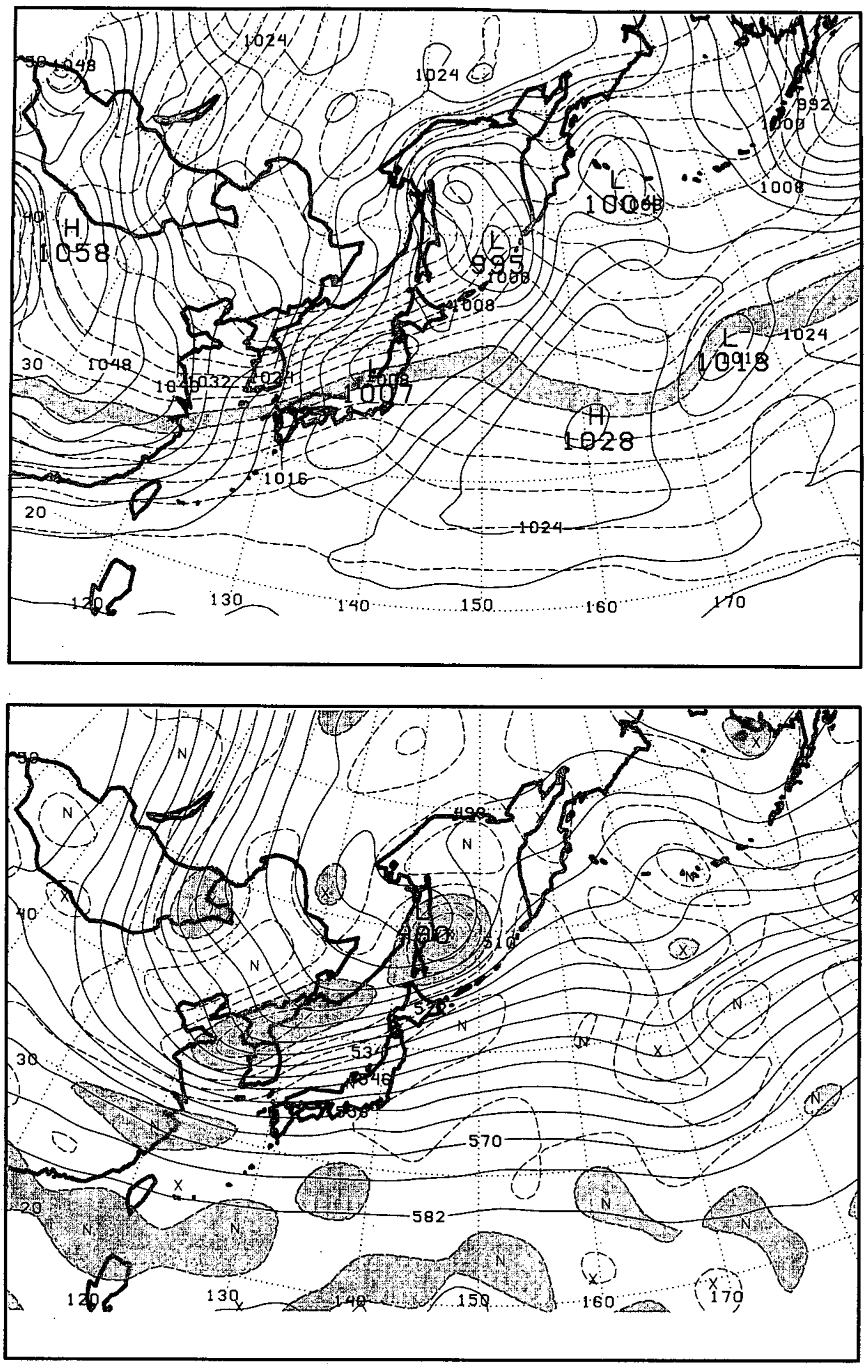

FIG. 5. For day 101.0, (a) sea level isobars (solid) at intervals of 4 mb, labeled with the tens and units digits, and contours of the thickness of the layer from 1000–500 mb (dashed), at intervals of 6 dam, with shading between the 534- and 540-dam isopleths. Centers of high and low pressure are denoted by H's and L's, respectively, and are labeled in millibars. (b) The 500-mb height contours (solid) at 6-dam intervals, labeled with tens and units digits and isopleths of absolute geostrophic vorticity (dashed) at intervals of 4×10^{-5} s^{-1}, with shading where the value is larger than 18 or smaller than 2 of these units. Highs and lows of height are denoted by H's and L's, respectively, and are labeled in dekameters.

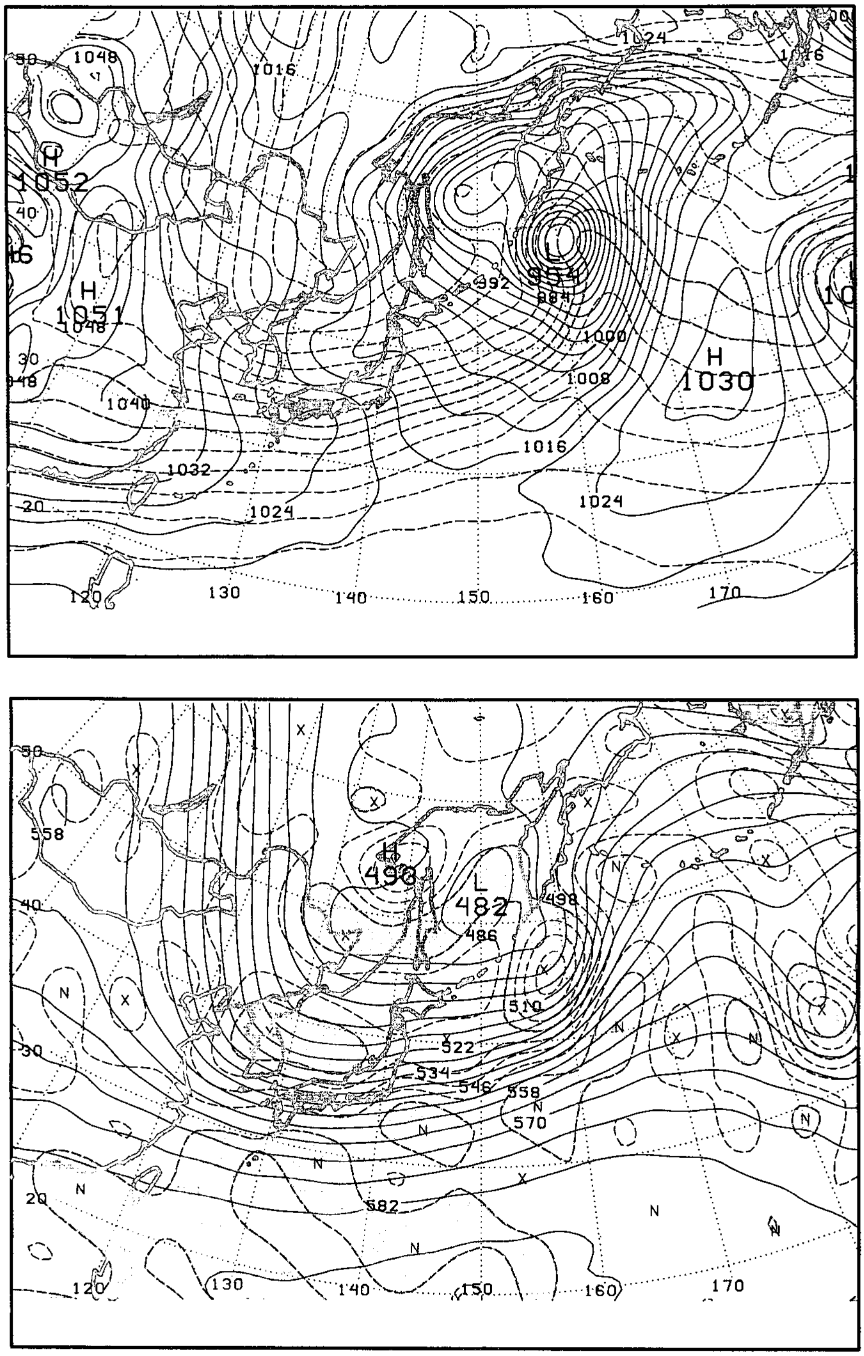

FIG. 6. Same as in Fig. 5 but for day 102.0. The heavy L's show the position of the surface low center at 12-h intervals from days 99.5 to 103.0. The heavy crosses show the position of the 500-mb vorticity center at 12-h intervals from days 99.0 to 103.0.

12 h (not shown). This final deepening must have been attributable to some mechanism other than the usual advection of vorticity or potential vorticity in the upper troposphere above the surface center. The latent heat release and the surface flux of heat are likely candidates, but we did not attempt a diagnosis of this occurrence.

A substantial low (not shown) that had moved eastward out of the map area on day 100.5, as well as the low that immediately preceded the cyclone under discussion, maintained a general northerly flow over the region of extreme cyclogenesis, thus keeping cold air over this region. Sanders and Davis (1988) showed that cold air thus positioned was favorable for especially great intensity of the following cyclone. In this respect the behavior of the model resembles that of the real atmosphere.

6. Conclusions

During a 180-day simulation of the cold season starting 1 October, the NCAR CCM2 closely resembled the observed atmosphere with respect to frequency, location, and intensity of explosive cyclogenesis.

Acknowledgments. This research was supported by the National Science Foundation under Grants ATM-9419411 and ATM-9318751. We are especially grateful to David Baumhefner, NCAR, for making the CCM2 output available to us.

REFERENCES

Hack, J. J., 1994: Parameterization of moist convection in the NCAR Community Climate Model (CCM2). *J. Geophys. Res.*, **99**, 5541–5568.

——, B. A. Boville, B. P. Briegleb, J. T. Kiehl, P. J. Rasch, and D. L. Williamson, 1993: A description of the NCAR Community Climate Model (CCM2). NCAR Tech. Note 382+STR, 108 pp. [Available from NCAR, P.O. Box 3000, Boulder, CO 80307-3000.]

Kiehl, J. T., R. J. Wolski, H. B. Briegleb, and V. Ramanathan, 1987: Documentation of radiation and cloud routines in the NCAR Community Climate Model (CCM1). NCAR Tech. Note NCAR/TN-288+IA. [Available from NCAR, P.O. Box 3000, Boulder, CO 80307-3000.]

Manabe, S., J. Smagorinsky, and R. F. Strickler, 1965: Simulated climatology of a general circulation model with a hydrologic cycle. *Mon. Wea. Rev.*, **93**, 769–798.

Press, W. H., S. A. Tuekolsky, W. T. Vetterling, and B. P. Flannery, 1992: *Numerical Recipes in Fortran: The Art of Scientific Computing.* 2d ed. Cambridge University Press, 963 pp.

Sanders, F., 1986: Explosive cyclogenesis in the west-central North Atlantic Ocean. Part I: Composite structure and mean behavior. *Mon. Wea. Rev.*, **114**, 1781–1794.

——, and J. R. Gyakum, 1980: Synoptic–dynamic climatology of the "bomb." *Mon. Wea. Rev.*, **108**, 1590–1606.

——, and C. A. Davis, 1988: Patterns of thickness anomaly for explosive cyclogenesis over the west-central North Atlantic Ocean. *Mon. Wea. Rev.*, **116**, 2725–2730.

Wadsworth, G. P., and J. G. Bryan, 1960: *An Introduction to Probability and Random Variables.* McGraw-Hill, 292 pp.

Williamson, D. H., J. T. Kiehl, V. Ramanathan, R. E. Dickinson, and J. J. Hack, 1987: Description of the NCAR Community Climate Model (CCM1). NCAR Tech. Note NCAR/TN285+STR, 112 pp. [Available from NCAR, P.O. Box 3000, Boulder, CO 80307-3000.]

Williamson, G. S., 1993: CCM2 datasets and circulation statistics. NCAR Tech. Note NCAR/TN-391+STR, 85 pp. [Available from NCAR, P.O. Box 3000, Boulder, CO 80307-3000.]